Published in final edited form as:
Nat Struct Mol Biol. 2010 June ; 17(6): 732–739. doi:10.1038/nsmb.1815.

hnRNP C promotes APP translation by competing with FMRP for *APP* mRNA recruitment to P bodies

Eun Kyung Lee[1], **Hyeon Ho Kim**[1], **Yuki Kuwano**[1], **Kotb Abdelmohsen**[1], **Subramanya Srikantan**[1], **Sarah S. Subaran**[2], **Marc Gleichmann**[3], **Mohammed R. Mughal**[3], **Jennifer L. Martindale**[1], **Xiaoling Yang**[1], **Paul F. Worley**[4], **Mark P. Mattson**[3], and **Myriam Gorospe**[1,*]

[1] Laboratory of Cellular and Molecular Biology, NIA-IRP, NIH, Baltimore, MD 21224, USA

[2] Confocal Imaging Facility, Research Resources Branch, NIA-IRP, NIH, Baltimore, MD 21224, USA

[3] Laboratory of Neurosciences, NIA-IRP, NIH Baltimore, MD, 21224, USA

[4] Department of Neuroscience, Johns Hopkins University School of Medicine, Baltimore, MD 20205, USA

Abstract

Amyloid precursor protein (APP) regulates neuronal synapse function and its cleavage product Aβ is linked to Alzheimer's disease. Here, we present evidence that RNA-binding proteins (RBPs) heterogeneous nuclear ribonucleoprotein (hnRNP) C and fragile-X mental retardation protein (FMRP) associate with the same *APP* mRNA coding region element and influence APP translation competitively and in opposite directions. Silencing hnRNP C increased FMRP binding to *APP* mRNA and repressed APP translation, while silencing FMRP enhanced hnRNP C binding and promoted translation. Repression of APP translation was linked to colocalization of FMRP and tagged *APP* mRNA within processing bodies (PBs); this colocalization was abrogated by hnRNP C overexpression or FMRP silencing. Our findings indicate that FMRP represses translation by recruiting *APP* mRNA to PBs, while hnRNP C promotes APP translation by displacing FMRP, thereby relieving the translational block.

INTRODUCTION

Amyloid precursor protein (APP) is a transmembrane protein implicated in synapse formation and synaptic plasticity[1–3]. The secreted extracellular domain of APP (sAPPα) has growth-factor properties and promotes neuritogenesis. Cleavage of APP by β- and γ-secretases releases neurotoxic peptides, including Aβ, whose accumulation is directly linked to the pathogenesis of neurodegenerative disorders such as Alzheimer's disease (AD). Several studies also support the notion that overproduction of APP underlies AD[4–8]. Elevated *APP* mRNA levels can result from altered APP transcription, although the specific transcription factors involved remain elusive[9–11]. By contrast, there is extensive evidence that APP expression is potently regulated by post-transcriptional mechanisms such as *APP* mRNA stabilization and APP translation[12–18], indicating that the regulation of *APP* mRNA metabolism is an important event in AD pathophysiology.

*Corresponding author: LCMB, NIA-IRP, NIH, 251 Bayview Blvd, Baltimore, MD 21224, USA, Tel: 410-558-8443; Fax: 410-558-8386, myriam-gorospe@nih.gov.

AUTHOR CONTRIBUTIONS

E.K.L., H.H.K., K.A., J.L.M., X.Y., M.P.M., and M. Gorospe designed the study E.K.L., H.H.K., Y. K., K.A., S.S., S.S.S., J.L.M., and X.Y. performed the experiments E.K.L., Y. K., M. Gleichmann, M.R.M., X.Y., P.F.W, and M.P.M. contributed key reagents E.K.L., M.P.M., and M.G. wrote the paper

Post-transcriptional processes are major mechanisms by which mammalian cells control gene expression[19]. Changes in mRNA turnover and translation rates are particularly important for altering the levels of expressed proteins[20]. These events are governed by two major types of *trans*-binding factors that interact with the mRNA: turnover- and translation-regulatory RNA-binding proteins (TTR RBPs) and noncoding (nc)RNAs such as microRNAs. TTR RBPs and ncRNAs bind to *cis* elements on the mRNA, frequently at the 5′- and 3′-untranslated regions (UTRs). APP expression was shown to be influenced by 3′UTR *cis*-elements that constitute the target sites of several microRNAs[12,13], as well as by TTR RBPs that increased *APP* mRNA stability (hnRNP C) or promoted *APP* mRNA decay (nucleolin)[14,15]. APP translation was also modulated by 5′UTR *cis*-elements, including an iron-responsive element (IRE) and an internal ribosome entry site (IRES)[16,17]. Additionally, APP translation was shown to be modulated by a TTR RBP that associated with a coding region (CR) *cis*-element and repressed APP translation, the fragile X mental retardation protein (FMRP)[18].

In a recent survey, we identified several RBPs that interacted with different regions of human *APP* mRNA. Among the novel interactions discovered, the RBP hnRNP C was found to bind to the same segment of the *APP* CR as did FMRP. We present evidence that hnRNP C promotes APP translation while FMRP represses it, and that the two RBPs interact with the *APP* CR in a competitive fashion. Moreover, repression of APP translation was linked to the colocalization of FMRP and a tagged *APP* RNA in processing bodies (PBs), where non-translating mRNAs assemble. These results link the repression of APP translation to the recruitment of the FMRP–*APP* mRNA complex to PBs, and further suggest that hnRNP C promotes APP translation by competing with FMRP, in turn blocking the recruitment of *APP* mRNA to PBs.

RESULTS

The *APP* coding region associates with RBPs hnRNP C and FMRP

To study the regulation of APP expression by RBPs, we silenced various TTR RBPs by transfecting the human neuroblastoma cell line BE2-M17 with the corresponding siRNAs. This initial survey (Supplementary Fig. 1) revealed that APP abundance was altered after lowering FMRP and hnRNP C. We first tested if FMRP and hnRNP C associated with the *APP* mRNA by immunoprecipitation of native ribonucleoprotein complexes (RNP IP analysis) followed by detection of the *APP* mRNA in the RNP complexes by using reverse transcription (RT) and quantitative (q)PCR amplification. As shown in Figure 1a (*top*) and in the Supplementary Figure 1, the *APP* mRNA was significantly enriched in both the hnRNP C and FMRP IPs (Fig. 1a, *bottom*), in keeping with previous reports that hnRNP C and FMRP associated with the *APP* mRNA[14,18]. Further studies were then conducted to identify the regions of interaction by testing biotinylated fragments of the *APP* mRNA (Fig. 1b and Supplementary Fig. 2). hnRNP C had affinity for the 3′UTR (segment G) and, unexpectedly, also for the *APP* CR (segment C) (Fig. 1a). While hnRNP C is predominantly nuclear, it is also readily detected in the cytoplasm, although in lower abundance (Supplementary Fig. 3).

Evidence that FMRP and hnRNP C interacted with fragment C in intact cells was sought by analysis of RNP crosslinking before lysis and IP (CLIP). CLIP analysis revealed the association of each RBP with *APP* fragment C in the cell (Fig. 1c), indicating that the RNPs detected in Figure 1a occurred in intact cells and did not arise from re-association of FMRP or hnRNP C with *APP* mRNA after membrane disruption. Since both hnRNP C and FMRP associated with fragment C (while other RBPs tested did not, Supplementary Fig. 2), we hypothesized the existence of a functional link between the two RBPs on the *APP* CR and set out to study this possibility.

hnRNP C and FMRP modulate *APP* mRNA translation

We first investigated whether hnRNP C and FMRP were directly involved in regulating APP expression by silencing hnRNP C or FMRP using small interfering (si)RNA, which effectively reduced hnRNP C and FMRP levels in BE2-M17 cells (Fig. 2a). Under these conditions, APP protein levels were markedly decreased in the hnRNP C siRNA group and strongly upregulated in the FMRP siRNA group (Fig. 2a). These changes did not arise from altered *APP* mRNA abundance (Fig. 2b) or protein turnover (not shown); instead, we postulated that APP translation could be influenced by these two RBPs.

The rate of APP translation was measured after incubation of BE2-M17 cells with ^{35}S-methionine and ^{35}S-cysteine for 15 min followed by APP IP to detect *de novo* synthesized APP; as shown, translation was reduced in the hnRNP C group and was elevated in the FMRP group (Fig. 2c). The relative association of *APP* mRNA with polyribosomes, an indirect measure of its translation, was studied by fractionating the cytoplasmic components on sucrose gradients; representative sucrose gradient profiles are shown in Figure 2d, *right* (and Supplementary Fig. 4). Fractionation was followed by measurement of the levels of *APP* mRNA (by RT-qPCR) in each fraction: untranslated (fractions 1 and 2), ribosome subunits and monosomes (fractions 3–5), low-molecular-weight polysomes (fractions 6–8), and high-molecular-weight polysomes (fractions 9–12). Compared with the distribution of *APP* mRNA in control siRNA cells (peaking at fraction 10), silencing hnRNP C shifted the *APP* mRNA distribution to lower parts of the gradient, with much of the *APP* mRNA peaking at fraction 8, in keeping with a reduction in APP translation in the hnRNP C siRNA population. Conversely, silencing FMRP increased the relative abundance of *APP* mRNA in the highest translating fraction (fraction 10), which contained 33% of the *APP* mRNA from Ctrl siRNA cells and 41% of *APP* mRNA from FMRP siRNA cells; these data reveal a greater proportion of large polysomes translating APP after silencing FMRP. FMRP and hnRNP C specifically altered the translational status of the *APP* mRNA, as the profiles for the mRNA encoding the housekeeping protein β-actin were quite similar among the silencing groups (Fig. 2d, *left*).

To further test the possibilities that FMRP reduced APP translation while hnRNP C promoted it, each RBP was overexpressed by transfection using plasmid vectors, then APP levels were measured. As shown, hnRNP C overexpression increased APP protein, but not *APP* mRNA levels (Fig. 2e; Supplementary Fig. 5), while FMRP overexpression decreased APP protein, but not *APP* mRNA levels (Fig. 2f; Supplementary Fig. 5). Together with the silencing data, these results indicate that FMRP functions as a repressor of APP translation in human neuroblastoma BE2-M17 cells (as previously shown in mouse neurons[18]) and further suggest that hnRNP C functions as an enhancer of APP translation.

Regulation of APP expression through 3′UTR fragment G and CR fragment C

Next, we sought to identify the regions of *APP* mRNA implicated in this translational control using reporter constructs. As hnRNP C associated prominently with the APP 3′UTR segment G (Fig. 1b), we first tested the contribution of this RNA region by preparing a construct that expressed a chimeric RNA containing *APP* fragment G at the 3′UTR (EGFP + 3′ UTR(G); Fig. 3a). When control and hnRNP C siRNA-transfected cells were compared, expression of the control *EGFP* reporter mRNA was unchanged but expression of *EGFP + 3′ UTR(G)* reporter mRNA was reduced in the hnRNP C siRNA group, as assessed both by Western blot analysis (Fig. 3b) and by fluorescence microscopy (Fig. 3c). This reduction was not due to a decrease in *EGFP + 3′ UTR(G)* mRNA abundance, since these levels remained unchanged, as measured using RT-qPCR (Fig. 3d). Instead, the altered EGFP expression appeared to be due to modest upregulation of EGFP translation in the presence of hnRNP C through the 3′UTR(G) sequence.

Since both hnRNP C and FMRP associated with segment C of the *APP* CR, we tested the contribution of their interaction at this RNA region by using a reporter construct in which region C was inserted in frame into the CR of EGFP (EGFP + CR(C)) (Fig. 4a). Expression of the control EGFP reporter protein was unchanged among the transfection groups. By contrast, expression of EGFP + CR(C) protein was lower in the hnRNP C siRNA group and was higher in the FMRP siRNA group, as tested both by Western blot analysis (Fig. 4b) and by fluorescence microscopy (Fig. 4c). As seen with the 3′UTR reporter (Fig. 3), the changes in EGFP + CR(C) protein levels were not due to altered *EGFP + CR(C)* mRNA abundance (Fig. 4d) and were instead attributed to altered translation rates in the hnRNP C and FMRP siRNA transfection groups. This notion was tested further by overexpressing hnRNP C, which enhanced reporter EGFP protein levels without significantly altering the levels of *EGFP* or *EGFP + CR(C)* mRNAs (Fig. 4e). On the other hand, FMRP overexpression lowered reporter EGFP protein levels but did not significantly alter the levels of *EGFP* or *EGFP + CR(C)* mRNAs (Fig. 4f). In sum, FMRP can reduce the translation of a reporter construct through *APP* CR(C) while hnRNP C can enhance translation strongly through the *APP* CR(C) and modestly through the *APP* 3′UTR(G).

hnRNP C and FMRP bind to *APP* mRNA competitively

As both hnRNP C and FMRP could associate with *APP* CR(C) but had opposite effects on *APP* mRNA levels, we postulated that hnRNP C and FMRP might compete for interaction with the *APP* mRNA. To test this hypothesis, we studied the binding of hnRNP C in cells expressing normal (control siRNA) or reduced (FMRP siRNA) levels of FMRP; as shown (Fig. 5a), silencing FMRP resulted in greater levels of the RNP complex (hnRNP C–*APP* mRNA) than were seen in cells with normal FMRP levels. Conversely, a comparison of cells expressing normal (control siRNA) or reduced levels of hnRNP C (hnRNP C siRNA) showed that the RNP complex (FMRP–*APP* mRNA) was higher in cells with silenced hnRNP C than in cells with normal hnRNP C levels (Fig. 5b). These findings were recapitulated using EGFP reporters: *EGFP + CR(C)* mRNA was significantly more enriched in hnRNP C IP samples after silencing FMRP (Fig. 5c), while the same reporter mRNA was more prominently associated with FMRP after silencing hnRNP C (Fig. 5d). To study the competition between FMRP and hnRNP C in a neurological disease model, we used mice lacking FMR1 (Fmr1 KO) [21]. As shown in Figure 5e, the steady-state abundance of mouse APP (mAPP) mRNA in whole-brain RNA was comparable between wild-type (WT) and Fmr1 KO mice. However, the interaction of hnRNP C with mouse mAPP mRNA was significantly more abundant in Fmr1 KO brain lysates than in WT brain lysates (Fig. 5f), associated with significantly higher expression of APP protein in the Fmr1 KO mice (Fig. 5g, in agreement with an earlier findings[18]). Collectively, these observations support the view that hnRNP C and FMRP compete for association with the *APP* CR and further indicate that translation increases if *APP* CR associates with hnRNP C, while it decreases if *APP* CR associates with FMRP.

FMRP recruits *APP* mRNA to processing bodies

Recently, several studies have shown that FMRP co-localizes with PBs, where non-translating mRNAs accumulate and can be sorted for transient storage or degradation[22–25]. First, we tested whether Argonaute (Ago) proteins, which function as translational repressors, were functionally linked to the inhibitory activity of FMRP. As shown in Figure 6a, FMRP overexpression increased significantly the association of *APP* mRNA with HA-tagged Ago1 and Ago2 proteins, which are PB-resident proteins. In keeping with the suppression of gene expression by Ago proteins, overexpression of HA-Ago1 or HA-Ago2 each reduced basal APP abundance, although it did not prevent the increase in APP levels that ensued silencing FMRP (Fig. 6b). FMRP and Ago associated by RNA-independent protein–protein interaction, as determined by IP followed by Western blot analysis in the presence of RNases (Fig. 6c). This analysis also revealed the interaction of FMRP with RCK, a component of PBs implicated in

translational repression[26] (Fig. 6c). It is important to note that FMRP did not repress APP translation in the absence of RCK, Ago1 or Ago2 (Supplementary Fig. 6). The distribution of FMRP and PBs was further studied by immunofluorescence, which revealed extensive colocalization of FMRP with Ago2, as well as with the PB markers Dcp1 and Rck (Fig. 6d). These data indicate that in human neuroblastoma BE2-M17 cells, FMRP is highly abundant in PBs.

To investigate directly whether the localization of FMRP in PBs is implicated in FMRP's repression of APP translation, we studied the subcellular localization of *APP* mRNA. First, we tested the presence of *APP* mRNA in PBs by performing anti-RCK RNP IP followed by RT-qPCR to detect *APP* mRNA. When FMRP is overexpressed, *APP* mRNA was significantly more abundant in RCK IP samples, suggesting that FMRP enhances the association of *APP* mRNA with PBs (Supplementary Fig. 7a). However, since not all RCK may be present in PBs, we sought to study the subcytoplasmic localization of *APP* mRNA in intact cells. To this end, we prepared reporter construct pMS2-APP (details in Methods), which expressed a chimeric RNA (*MS2-APP*) comprising the *APP* CR(C) segment and 24 tandem MS2 RNA hairpins (Fig. 7a). Co-transfection of pMS2-APP together with plasmid pMS2-YFP, which expressed the chimeric fluorescent protein MS2-YFP with a nuclear localization signal (NLS; see Methods), allowed us to track the subcellular localization of the chimeric *MS2-APP* RNA (as the MS2-YFP–*MS2-APP* complex) as well as the control *MS2* RNA (as the MS2-YFP–*MS2* complex) by confocal microscopy. Despite potential artifacts, the MS2 system has been used successfully to track the subcellular localization of RNAs[27] As shown in Figure 7b (*left*), the control *MS2* RNA appeared to be exclusively nuclear in all of the transfected cells, due to the presence of the NLS (Fig. 7a). By contrast, some *MS2-APP* RNA was retained the cytoplasm with a punctate pattern, colocalizing to some extent (but not exclusively) with RCK signals; colocalization results in yellow signals in the merged images (Fig. 7b, *right*, arrowheads, and Supplementary Fig. 7). The colocalization of MS2-YFP–*MS2-APP* and RCK signals was lost in the transfected cells when hnRNP C was overexpressed (Fig. 7c *right*) but was seen in the corresponding control cells (Fig. 7c *left*). Similarly, the colocalization of MS2-YFP–*MS2-APP* and RCK signals was lost when FMRP was silenced (Fig. 7d *middle*) but was seen in the corresponding control cells (Fig. 7d *left*) and in cells with silenced hnRNP C (Fig. 7d *right*). Together, these results support the view that FMRP represses *APP* mRNA translation at least in part by recruiting the transcript to PBs. According to this paradigm, hnRNP C promotes translation by competing for interaction of FMRP with the *APP* CR, thereby preventing the localization of *APP* mRNA at PBs (Fig. 8).

DISCUSSION

hnRNP C and FMRP were found to compete for binding to the CR of *APP* mRNA in a competitive manner and modulated APP translation in opposite directions: hnRNP C enhanced APP translation, while FMRP repressed it. These conclusions were reached by analyzing both the endogenous *APP* mRNA and reporter constructs bearing the ~120-nt *APP* CR fragment C where binding by these RBPs was mapped. As shown, silencing FMRP promoted binding of hnRNP C to *APP* mRNA and enhanced APP translation, while silencing hnRNP C increased FMRP binding to *APP* mRNA and lowered APP translation. Accordingly, FMRP overexpression inhibited APP translation and hnRNP C overexpression increased it (Figs. 2, 4, 5). Our results confirm and expand upon the findings of Westmark and Malter, who showed that FMRP bound to a G-rich (G-quartet-like) CR segment in the *APP* CR and repressed APP translation in mouse neurons[18]. The authors further showed that the inhibitory interaction of FMRP with the *APP* CR was relieved after treatment with DHPG, an agonist of the metabotropic glutamate receptor (mGluR)[18].

FMRP was previously shown to suppress strongly and specifically the translation of several mRNAs in rabbit reticulocyte lysates and in microinjected oocytes[28]. *En masse* analysis of FMRP RNP complexes revealed altered translational profiles for many target transcripts[29]; FMRP was generally found to bind target mRNAs in the 5′- and 3′-UTRs[29,30]. The precise mechanisms of translational repression by FMRP are unclear, but the RBP appears to prevent the assembly of 80S on target mRNAs, and its phosphorylation correlates with its presence in stalled polyribosomes[27,31–33]. Earlier studies also provided evidence that FMRP associated with the RNAi effector complex RISC, suggesting a link between FMRP and the inhibition of translation through the microRNA pathway[34–37]. More recently, FMRP was implicated in the assembly of stress granules (SGs), which form transiently in response to cellular damage; this finding is potentially relevant to the translational repression by FMRP, since SGs are believed to contain untranslated mRNAs that are subject to RNP remodelling to modulate their subsequent turnover and translation rates[38]. Our findings support the view that FMRP represses APP translation at least in part by reducing the rate of translation initiation (since a larger population of heavy polyribosomes is seen after silencing FMRP, Fig. 2d), by reducing nascent APP translation (Fig. 2c), and translation of a reporter RNA (Fig. 4) and by recruiting a tagged *APP* RNA (containing CR(C)) to PBs (Figs. 6d and 7), where non-translating mRNAs accumulate[22–25]. It remains to be seen whether FMRP also inhibits APP translation by stalling preinitiation complexes or by recruiting the *APP* mRNA onto SGs, RISC, or other cellular machineries.

The mechanisms whereby hnRNP C promotes APP translation are also unclear at present. hnRNP C1/C2 was previously suggested to promote polyadenylation and enhanced the initiation of Unr (upstream of N-Ras) translation during mitosis[39,40]. The promotion of Unr translation by hnRNP C was shown to be mediated by an internal ribosome entry site (IRES), antagonizing the polypyrimidine tract-binding protein (PTB). Interestingly, the *APP* mRNA also has a functional IRES in the 5′UTR[17]. Although it lies several hundred nucleotides away from the G-rich region of association with hnRNP C, it will be interesting to study if the promotion of APP translation by hnRNP C is related to the APP IRES. Nonetheless, our results indicate that hnRNP C overexpression increases the initiation of *APP* mRNA translation (Fig. 2d), the overall *de novo* APP translation (Fig. 2c), the translation of a reporter mRNA (Fig. 4), and the recruitment of tagged APP RNA to PBs (Fig. 7). In light of our results that hnRNP C promotes APP translation by competing with FMRP for binding to the *APP* CR, it will also be important to study whether hnRNP C competes with FMRP in the binding of other FMRP target mRNAs identified by Brown and coworkers[29], and whether hnRNP C stimulates their translation.

How PBs repress the translation of resident mRNAs is not fully understood. However, PBs contain many translational repressors, including decapping enzymes (DCP1, DCP2), mRNA deadenylation factors (e.g. the CCR4–CAF-1–Not complex), activators of decapping (Dhh1/RCK/p54, Pat1, Scd6/RAP55, Edc3, the Lsm1-7 complex), and exonucleases (e.g. XRN-1)[41–43]. FMRP interacts with Ago proteins and the microRNA pathway suggesting that microRNAs could also participate in controlling APP translation. MicroRNAs, such as miR-106a/b, miR-520c, miR-20a and miR-17-5p, associate with the APP 3′UTR and contribute to repressing its translation[12,13]. It is not known at this time whether such interactions are functionally linked to the actions of FMRP or hnRNP C, although these microRNAs interact with regions outside of CR segment C. Also awaiting experimental analysis is whether stresses can alter the binding of any of the factors (RBPs, microRNAs) that interact with the *APP* mRNA.

In studies that examined the APP 3′UTR, hnRNP C and nucleolin were shown to bind to a 29-nt sequence in the APP 3′UTR and increased *APP* mRNA stability in rabbit reticulocyte lysates[14]. In agreement with these findings, we also observed extensive binding of hnRNP C

to the APP 3′UTR (Fig. 1); however, we did not observe significant differences in *APP* mRNA levels or stability under the conditions of our study, perhaps because the two cell types differ in this respect (Fig. 3 and data not shown). Several other RBPs were also found to influence APP expression. HuD bound the *APP* mRNA at the 3′UTR (Supplementary Fig. 1) and silencing lowered *APP* mRNA and protein levels (Supplementary Fig. 1 and data not shown). However, given the long half-life of *APP* mRNA ($t_{1/2}$ >12 h, (ref. [44] and data not shown)), it seems that HuD may regulate APP expression indirectly, perhaps by affecting the expression of a transcription factor that controls APP gene transcription.

In closing, RBPs such as FMRP and hnRNP C together with microRNAs that interact with the *APP* mRNA are emerging as pivotal post-transcriptional regulators of APP production. These factors help to ensure that APP is expressed in the correct abundance, as dictated by the developmental and metabolic state of the cell. Given the multiplicity of factors controlling the turnover and translation of *APP* mRNA, further studies are warranted to elucidate their complex interactions. Although the physiologic function of APP is not understood completely, the levels of APP directly impact upon the levels of processed Aβ. Thus, a thorough knowledge of the control of APP levels is critical in order to understand how AD arises and to develop effective AD interventions.

METHODS

Cell culture, transfection, small interfering (si)RNAs and plasmids

We cultured human neuroblastoma BE2-M17 cells in Opti-MEM and Dulbecco's modified essential medium (Invitrogen) supplemented with 10% FBS. We transfected small interfering (si)RNAs targeting hnRNP C and FMRP (sc-35577 and sc-36870, Santa Cruz Biotechnology) and control (Ctrl) siRNA (Qiagen), comprising three pooled siRNAs without known off-target effects, at 20 nM final concentration using Oligofectamine (Invitrogen) and analyzed cells 48 h later. We constructed reporter plasmids by inserting fragments from the APP 3′UTR (2232–2635) and CR (901–1020) into plasmid pEGFP-C1 (BD Bioscience)[45]. To overexpress hnRNP C, we prepared an expression vector by amplifying the hnRNP C CR (NM_031314.2) using PC and ligating it at BamHI and XhoI sites of plasmid pcDNA3 using primers ACTTAGGATCCATGGCCAGCAACGTTACC and ACTCATCTCGAGTTAAGAGTCATCCTCGCCATTG. Dr. R. Willemsen (Erasmus MC, The Netherlands) kindly provided pEGFP-FMRP. We obtained HA-Ago1 and HA-Ago2 from Addgene. We prepared pMS2-APP from plasmid pSL-MS2(24X). Dr. R. H. Singer generously provided plasmids pSL-MS2 and pMS2-YFP[25]. We inserted MS2-YFP cDNA into plasmid pcDNA3 to increase expression levels (see below). We ligated the MS2 hairpin sequence (24 repeats) from pSL-MS2 at EcoRI and EcoRV sites and APP CR(C) at the XhoI site of pcDNA3. We used Lipofectamine 2000 (Invitrogen) for plasmid transfections.

Western blot analysis

We used RIPA buffer to prepare whole-cell lysates, separated them by electrophoresis in SDS-containing polyacrylamide gels, and transferred them onto PVDF membranes (Millipore). We used primary antibodies that recognized APP (Calbiochem), GFP (Santa Cruz Biotechnology), FMRP (Chemicon) or β-actin (Abcam), incubated the blots with the appropriate secondary antibodies conjugated with HRP (GE Healthcare) and detected the protein signals using enhanced luminescence (GE Healthcare).

RNA analysis

We used Triazol (Invitrogen) to prepare total RNA directly from cells or after immunoprecipitation (IP) from cellular RNA–protein complexes obtained by IP (using anti-FMRP (Abcam), anti-hnRNP C (Santa Cruz Biotechnology) or IgG antibodies), as described

below and in Ref. [46]. After reverse transcription (RT) using random hexamers and SSII reverse transcriptase (Invitrogen), we assayed the abundance of transcripts by real-time, quantitative PCR (qPCR) analysis using SYBR Green PCR master mix (Applied Biosystems) and gene-specific primer sets: GCCAAAGAGACATGCAGTGA and AGTCATCCTCCTCCGCATC for APP mRNA, TGCACCACCAACTGCTTAGC and GGCATGGACTGTGGTCATGAG for GADPH mRNA, and GGACTTCGAGCAAGAGATGG and AGCACTGTGTTGGCGTACAG for β-actin mRNA.

Immunoprecipitation assays

We prepared whole-cell lysates by incubating cells in RIPA buffer for 10 min on ice followed by centrifugation at 10,000 × g for 15 min at 4°C. We incubated the supernatants with protein A-Sepharose beads coated with primary antibody or control IgG (Santa Cruz Biotechnology) with or without RNaseT (Invitrogen) for 16 h. After washing the beads with RIPA buffer, we assayed the complexes by western blot analysis as described above.

Using whole-cell extracts, we performed IP of native RNP complexes (RNP IP analysis) as described[46] using primary antibodies (anti-hnRNP C or control IgG, Santa Cruz Biotechnology); after washes and digestion with DNase I and Proteinase K, we analyzed the RNA in the IP samples by RT-qPCR using the primers described above. We performed IP of crosslinked RNP complexes as described[47]. After RNase T1 digestion, we isolated RNA and analyzed it by RT-qPCR using primers that amplified segment C of the coding region (below).

Mouse brain analysis

We harvested whole brains from WT (4 female, 1 male) or Fmr1 KO (5 female) FvB mice[21], 4–5 months of age. To prepare brain homogentes, we used PEB buffer containing RNAse-OUT and 1X protease inhibitor cocktail, followed by centrifugation at 13,000 rpm for 30 min at 4 °C. We incubated the lysates (2 mg aliquots) with beads that were pre-coated with antibody (15 μg anti-hnRNP C or IgG) for 2 h at 4 °C. Subsequent steps are as described above.

Biotin pulldown assay

We prepared PCR templates to synthesize biotinylated transcripts spanning the APP mRNA (NM_201414). Forward primers contained the T7 RNA polymerase promoter sequence (CCAAGCTTCTAATACGACTCACTATAGGGAGA [T7]):

APP 5′UTR 51–190 (A): [T7]TTCCTCGGCAGCGGTAGGCGAGA and ACCCTGCGCGGGGCACCGAGT

APP CR 741–850 (B): [T7]GAGTTTGTGTGTTGCCCACTG and GAGTTTGTGTGTTGCCCACTG

APP CR 901–1020 (C): [T7]AGGTGGAAGAAGAAGAAGCCGAT and TGGTGGTGGCAATGCTGGTGGT

APP CR 1060–1205 (D): [T7]TTCCTACAACAGCAGCCAGT and TTCTCTCATGACCTGGGACATTCT

3′UTR 2283–2380 (E): [T7]ACCCCCGCCACAGCAGCCTCT and CGGGTTTGTTTCTTCCCACAT

3′UTR 2436–2545 (F): [T7]GCCTGAACTTGAATTAATCCACA and CAGCTAAATTCTTTACAGTACACA

3′UTR 2332–2635 (G): [T7]CTACCCATCGGTGTCCATTTATAG and GGGTCACAAACCACAAGAA

3′UTR 2618–3317 (H): [T7]TCTTGTGGTTTGTGACCCAATTAAG and CATGCCTTCCTCATCCCCTTA.

We tested biotinylated transcripts as previously explained[46].

Fractionation of polyribosomes

After silencing hnRNP C or FMRP for 48 h, we preincubated cells with cycloheximide (100 μg ml^{-1}, 15 min) and lysed them with PEB (polysome extraction buffer) containing 20 mM Tris-HCl at pH 7.5, 100 mM KCl, 5 mM $MgCl_2$ and 0.5% NP-40. We fractionated the cytoplasmic lysates by ultracentrifugation through 10–50% linear sucrose gradients and obtained 12 fractions for RNA extraction and RT-qPCR analysis, as described[48].

Analysis of *de novo* translation

We studied nascent translation of APP and GAPDH as described[48]. After incubation of BE2-M17 cells with 1 mCi L-[^{35}S] methionine and L-[^{35}S]cysteine (Easy Tag ™EXPRESS, NEN/Perkin Elmer, Boston, MA) per 60-mm plate for 15 min, cells were lysed in RIPA buffer (10 mM Tris-HCl [pH 7.4], 150 mM NaCl, 1% NP-40, 1 mM EDTA, 0.1% SDS, and 1 mM DTT). Following IP with anti-IgG1 (BD Pharmingen), anti-APP (Calbiochem) or anti-GAPDH antibodies (Santa Cruz Biotechnology), we washed the reaction beads in RIPA buffer, resolved the IP material by SDS-PAGE, transferred onto PVDF filters, and visualized and quantified it with a PhosphorImager (Molecular Dynamics).

Immunofluorescence and confocal microscopy

After transfection of plasmids or siRNAs, we fixed cells with 2% formaldehyde, permeabilized them with 0.2% Triton X-100, blocked with 5% BSA, and incubated them with primary antibodies recognizing Dcp1a (Abcam), RCK, EGFP or HA (Santa Cruz Biotechnology). We then used Alexa 488- or Alexa 568-conjugated secondary antibodies (Invitrogen) to detect primary antibody–antigen complexes with different color combinations as needed. We acquired the images using Axio Observer microscope (ZEISS) with AxioVision 4.7 Zeiss image processing software or with LSM 510 Meta (ZEISS). We acquired confocal microscopy images with *Z*-sectioning mode with 15 slices and 0.4 μm spacing and merged them using maximum intensity.

Supplementary Material

Refer to Web version on PubMed Central for supplementary material.

Acknowledgments

This research was supported by the National Institute on Aging-Intramural Research Program, National Institutes of Health. P.F.W. is suppported by DA00266. We thank F.E. Indig (Confocal Imaging Facility, NIA) and M.H. Dehoff (Johns Hopkins University School of Medicine) for assistance with experiments.

Abbreviations

APP	amyloid precursor protein
CR	coding region
FMRP	fragile X mental retardation protein
hnRNP	heterogeneous nuclear ribonucleoprotein
PBs	processing bodies

TTR RBP	translation and turnover regulatory RNA-binding protein
UTR	untranslated region

References

1. Torroja L, Packard M, Gorczyca M, White K, Budnik V. The Drosophila beta-amyloid precursor protein homolog promotes synapse differentiation at the neuromuscular junction. J Neurosci 1999;19:7793–7803. [PubMed: 10479682]
2. Mattson MP. Cellular actions of beta-amyloid precursor protein and its soluble and fibrillogenic derivatives. Physiol Rev 1997;77:1081–1132. [PubMed: 9354812]
3. Yang G, Gong YD, Gong K, Jiang WL, Kwon E, Wang P, Zheng H, Zhang XF, Gan WB, Zhao NM. Reduced synaptic vesicle density and active zone size in mice lacking amyloid precursor protein (APP) and APP-like protein 2. Neurosci Lett 2005;384:66–71. [PubMed: 15919150]
4. Rumble B, Retallack R, Hilbich C, Simms G, Multhaup G, Martins R, Hockey A, Montgomery P, Beyreuther K, Masters CL. Amyloid A4 protein and its precursor in Down's syndrome and Alzheimer's disease. New Engl J Med 1989;320:1446–1452. [PubMed: 2566117]
5. Hardy J, Selkoe DJ. The amyloid hypothesis of Alzheimer's disease: progress and problems on the road to therapeutics. Science 2002;297:353–356. [PubMed: 12130773]
6. Cohen ML, Golde TE, Usiak MF, Younkin LH, Younkin SG. In situ hybridization of nucleus basalis neuron shows increased beta-amyloid mRNA in Alzheimer's disease. Proc Natl Acad Sci USA 1988;84:1227–1231. [PubMed: 3277188]
7. Higgins GA, Oyler GA, Neve RL, Chen KS, Gage FH. Altered levels of Amyloid protein precursor transcripts in the basal forebrain of behaviorally impaired aged rats. Proc Natl Acad Sci USA 1990;87:3032–3036. [PubMed: 1970179]
8. Buckland P, Tidmarsh S, Spurlock G, Kaiser F, Yates M, O'Mahony G, McGuffin P. Amyloid precursor protein mRNA levels in the mononuclear blood cells of Alzheimer's and Down's patients. Mol Brain Res 1993;18:316–320. [PubMed: 8326826]
9. Theuns J, Brouwers N, Engelborghs S, Sleegers K, Bogaerts V, Corsmit E, De Pooter T, van Duijn CM, De Deyn PP, Van Broeckhoven C. Promoter mutations that increase amyloid precursor-protein expression are associated with Alzheimer disease. Am J Hum Genet 2006;78:936–946. [PubMed: 16685645]
10. Lv H, Jia L, Jia J. Promoter polymorphisms which modulate APP expression may increase susceptibility to Alzheimer's disease. Neurobiol Aging 2008;29:194–202. [PubMed: 17112637]
11. Wang PL, Niidome T, Akaike A, Kihara T, Sugimoto H. Rac1 inhibition negatively regulates transcriptional activity of the amyloid precursor protein gene. J Neurosci Res 2009;87:2105–2114. [PubMed: 19267423]
12. Patel N, Hoang D, Miller N, Ansaloni S, Huang Q, Rogers JT, Lee JC, Saunders AJ. MicroRNAs can regulate human APP levels. Mol Neurodegener 2008;3:10. [PubMed: 18684319]
13. Hébert SS, Horré K, Nicolaï L, Bergmans B, Papadopoulou AS, Delacourte A, De Strooper B. MicroRNA regulation of Alzheimer's Amyloid precursor protein expression. Neurobiol Dis 2009;33:422–428. [PubMed: 19110058]
14. Rajagopalan LE, Westmark CJ, Jarzembowski JA, Malter JS. hnRNP C increases amyloid precursor protein (APP) production by stabilizing APP mRNA. Nucleic Acids Res 1998;26:3418–3423. [PubMed: 9649628]
15. Westmark CJ, Malter JS. Extracellular-regulated kinase controls beta-amyloid precursor protein mRNA decay. Brain Res Mol Brain Res 2001;90:193–201. [PubMed: 11406297]
16. Rogers JT, et al. An Iron-responsive Element Type II in the 5′-untranslated region of the Alzheimer's amyloid precursor protein transcript. J Biol Chem 2002;277:45518–45528. [PubMed: 12198135]
17. Beaudoin ME, Poirel VJ, Krushel LA. Regulating amyloid precursor protein synthesis through an internal ribosomal entry site. Nucl Ac Res 2008;36:6835–6847.
18. Westmark CJ, Malter JS. FMRP mediates mGluR5-dependent translation of amyloid precursor protein. PLoS Biology 2007;5:629–639.

19. Orphanides G, Reinberg D. A unified theory of gene expression. Cell 2002;108:439–451. [PubMed: 11909516]
20. Moore MJ. From birth to death: the complex lives of eukaryotic mRNAs. Science 2005;309:1514–1518. [PubMed: 16141059]
21. Zalfa F, Giorgi M, Primerano B, Moro A, Di Penta A, Reis S, Oostra B, Bagni C. The fragile X syndrome protein FMRP associates with BC1 RNA and regulates the translation of specific mRNAs at synapses. Cell 2003;112:317–327. [PubMed: 12581522]
22. Parker R, Sheth U. P bodies and the control of mRNA translation and degradation. Mol Cell 2007;25:635–646. [PubMed: 17349952]
23. Barbee SA, et al. Staufen- and FMRP-containing neuronal RNPs are structurally and functionally related to somatic P bodies. Neuron 2006;52:997–1009. [PubMed: 17178403]
24. Eulalio A, Behm-Ansmant I, Izaurralde E. P bodies: at the crossroads of post-transcriptional pathways. Nat Rev Mol Cell Biol 2007;8:9–22. [PubMed: 17183357]
25. Balagopal V, Parker R. Polysomes, P bodies and stress granules: states and fates of eukaryotic mRNAs. Curr Opin Cell Biol 2009;21:403–408. [PubMed: 19394210]
26. Chu CY, Rana TM. Translation Repression in Human Cells by MicroRNA-Induced Gene Silencing Requires RCK/p54. PLoS Biol 2008;4:1122–1136.
27. Fusco D, Accornero N, Lavoie B, Shenoy SM, Blanchard JM, Singer RH, Bertrand E. Single mRNA molecules demonstrate probabilistic movement in living mammalian cells. Curr Biol 2003;13:161–167. [PubMed: 12546792]
28. Laggerbauer B, Ostareck D, Keidel EM, Ostareck-Lederer A, Fischer U. Evidence that fragile X mental retardation protein is a negative regulator of translation. Hum Mol Genet 2001;10:329–338. [PubMed: 11157796]
29. Brown V, et al. Microarray identification of FMRP-associated brain mRNAs and altered mRNA translational profiles in fragile X syndrome. Cell 2001;107:477–487. [PubMed: 11719188]
30. Todd PK, Mack KJ, Malter JS. The fragile X mental retardation protein is required for type-I metabotropic glutamate receptor dependent translation of PSD-95. Proc Natl Acad Sci USA 2003;100:14374–14378. [PubMed: 14614133]
31. Ceman S, O'Donnell WT, Reed M, Patton S, Pohl J, Warren ST. Phosphorylation influences the translation state of FMRP-associated polyribosomes. Hum Mol Genet 2003;12:3295–3305. [PubMed: 14570712]
32. Zalfa F, Achsel T, Bagni C. mRNPs, polysomes or granules: FMRP in neuronal protein synthesis. Curr Opin Neurobiol 2006;16:265–269. [PubMed: 16707258]
33. Zukin RS, Richter JD, Bagni C. Signals, synapses, and synthesis: how new proteins control plasticity. Front Neural Circuits 2009;3:14. [PubMed: 19838324]
34. Caudy AA, Myers M, Hannon GJ, Hammond SM. Fragile X-related protein and VIG associate with the RNA interference machinery. Genes Dev 2002;16:2491–2496. [PubMed: 12368260]
35. Ishizuka A, Siomi MC, Siomi H. A Drosophila fragile X protein interacts with components of RNAi and ribosomal proteins. Genes Dev 2002;16:2497–2508. [PubMed: 12368261]
36. Jin P, Alisch RS, Warren ST. RNA and microRNAs in fragile X mental retardation. Nat Cell Biol 2004;6:1048–1053. [PubMed: 15516998]
37. Jin P, Zarnescu DC, Ceman S, Nakamoto M, Mowrey J, Jongens TA, Nelson DL, Moses K, Warren ST. Biochemical and genetic interaction between the fragile X mental retardation protein and the microRNA pathway. Nat Neurosci 2004;7:113–117. [PubMed: 14703574]
38. Didiot MC, Subramanian M, Flatter E, Mandel JL, Moine H. Cells lacking the fragile X mental retardation protein (FMRP) have normal RISC activity but exhibit altered stress granule assembly. Mol Biol Cell 2009;20:428–437. [PubMed: 19005212]
39. Zhao X, Oberg D, Rush M, Fay J, Lambkin H, Schwartz S. A 57-nucleotide upstream early polyadenylation element in human papillomavirus type 16 interacts with hFip1, CstF-64, hnRNP C1/C2, and polypyrimidine tract binding protein. J Virol 2005;79:4270–4288. [PubMed: 15767428]
40. Schepens B, Tinton SA, Bruynooghe Y, Parthoens E, Haegman M, Beyaert R, Cornelis S. A role for hnRNP C1/C2 and Unr in internal initiation of translation during mitosis. EMBO J 2007;26:158–169. [PubMed: 17159903]

41. Ingelfinger D, Arndt-Jovin DJ, Lührmann R, Achsel T. The human LSm1-7 proteins colocalize with the mRNA-degrading enzymes Dcp1/2 and Xrnl in distinct cytoplasmic foci. RNA 2002;8:1489–1501. [PubMed: 12515382]

42. van Djk E, Cougot N, Meyer S, Babajko S, Wahle E, Séraphin B. Human Dcp2: a catalytically active mRNA decapping enzyme located in specific cytoplasmic structures. EMBO J 2002;21:6915–6924. [PubMed: 12486012]

43. Cougot N, Babajko S, Séraphin B. Cytoplasmic foci are sites of mRNA decay in human cells. J Cell Biol 2004;165:31–40. [PubMed: 15067023]

44. Rajagopalan LE, Malter JS. Growth factor-mediated stabilization of amyloid precursor protein mRNA is mediated by a conserved 29-nucleotide sequence in the 3′untranslated region. J Neurochem 2000;74:52–59. [PubMed: 10617105]

45. Abdelmohsen K, Srikantan S, Kuwano Y, Gorospe M. miR-519 reduces cell proliferation by lowering RNA-binding protein HuR levels. Proc Natl Acad Sci USA 2008;105:20297–20302. [PubMed: 19088191]

46. Abdelmohsen K, et al. Phosphorylation of HuR by Chk2 regulates SIRT1 expression. Mol Cell 2007;25:543–557. [PubMed: 17317627]

47. Jensen KB, Darnell RB. CLIP: crosslinking and immunoprecipitation of in vivo RNA targets of RNA-binding proteins. Methods Mol Biol 2008;488:85–98. [PubMed: 18982285]

48. Kuwano Y, Kim HH, Abdelmohsen K, Pullmann R Jr, Martindale JL, Yang X, Gorospe M. MKP-1 mRNA stabilization and translational control by RNA-binding proteins HuR and NF90. Mol Cell Biol 2008;28:4562–4575. [PubMed: 18490444]

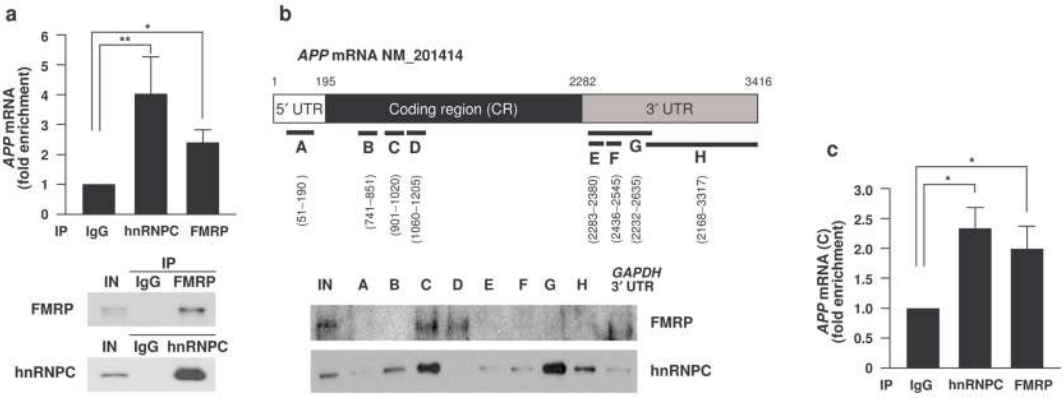

Figure 1. hnRNP C and FMRP interact with the CR of *APP* mRNA

(a) RNP IP analysis to study the enrichment of *APP* mRNA in samples obtained after IP of hnRNP C or FMRP (*top*) as detected by RT-qPCR analysis of *APP* mRNA and loading control *GAPDH* mRNA. *Bottom*, IP followed by Western blot analysis of FMRP and hnRNP C in the samples used for RNP IP analysis. The IgG sample was included to assess background binding to IP reagents; IN, input. **(b)** *Top*, schematic of the *APP* mRNA depicting the 5′UTR, CR, and 3′UTR, as well as the different segments that were tested by biotin pulldown assays and the nucleotide positions spanned by each fragment. *Bottom*, after incubation with the biotinylated RNAs indicated, the association of RBPs hnRNP C and FMRP was tested by Western blot analysis; biotinylated GAPDH 3′UTR was included as negative control. IN, input (10 μg lysate). **(c)** CLIP analysis of the interaction of hnRNP C and FMRP with segment C of *APP* CR. Data in (a) and (c) are shown as means +s.d. from 3 independent experiments; *, $p<0.05$; **, $p<0.01$.

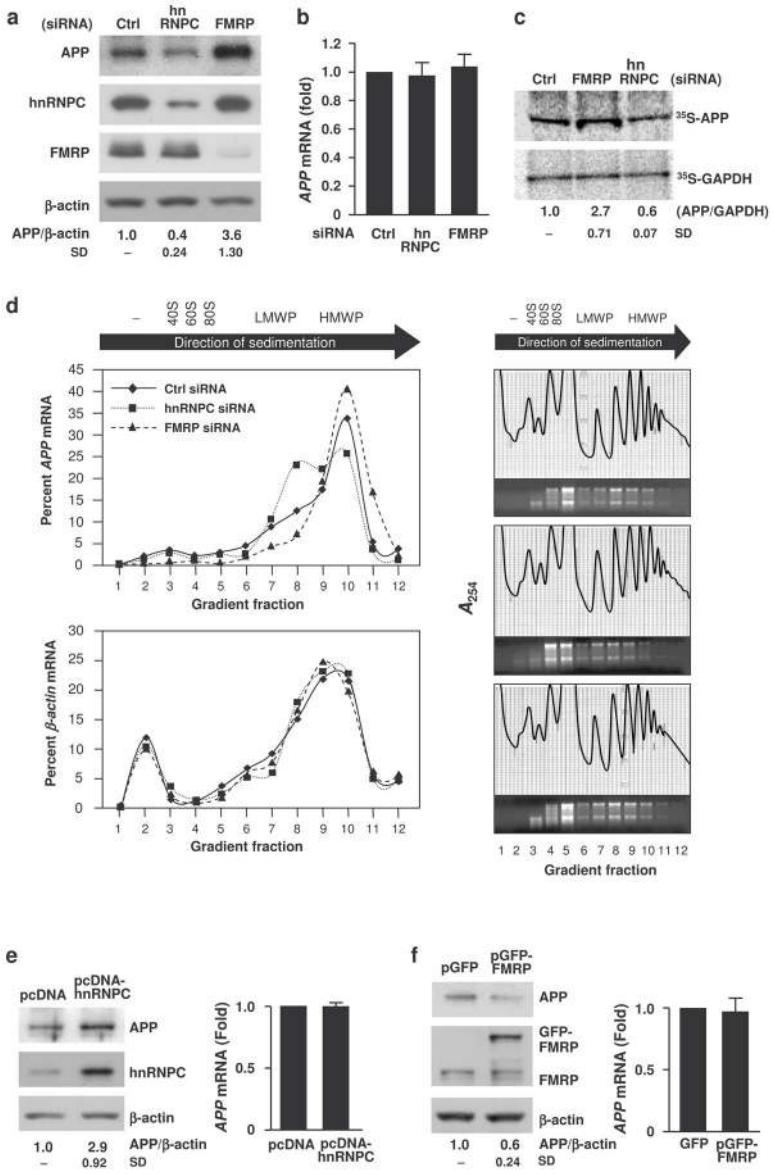

Figure 2. Effect of silencing hnRNP C and FMRP on APP expression

(a) 48 h after transfection of BE2-M17 cells with either control (Ctrl) siRNA or siRNAs directed towards hnRNP C or FMRP, the levels of APP, hnRNP C, FMRP, and loading control β-actin were assessed by Western blot analysis. Signals were quantified by densitometry and shown as the ratio of APP/β-actin. **(b)** The levels of *APP* mRNA in cells with silenced hnRNP C or FMRP were quantified by RT-qPCR and normalized to *GAPDH* mRNA. **(c)** *De novo* APP or GAPDH biosynthesis was assessed by APP or GAPDH IP 48 h after transfection of the indicated siRNAs. (details in Methods). **(d)** Lysates prepared from cells that were transfected as described in (a) were fractionated through sucrose gradients (*right*) and the relative distribution of *APP* mRNA (*top*) and housekeeping *β-actin* mRNA (*bottom*) was studied by RT-qPCR analysis of RNA in each of 10 gradient fractions. Arrow indicates the direction of sedimentation; –, fractions with no ribosomal components, 40S and 60S, small and large ribosome subunits, respectively; 80S, monosomes; LMWP and HMWP, low- and high-molecular-weight polysomes, respectively. Below each profile, 18S and 28S rRNA were visualized by ethidium bromide staining of RNA aliquots from each fraction. Data are

representative of 3 independent experiments. **(e,f)** BE2-M17 cells were transfected with either an empty vector control or an RBP expression vector (pcDNA and pcDNA-hnRNP C (e)) or (pGFP and pGFP-FMRP (f)). In each transfection group, APP protein levels were assessed by Western blot analysis and quantified by densitometry using β-actin for normalization (*left*); *APP* mRNA levels in each group were measured by RT-qPCR using *GAPDH* mRNA for normalization (*right*). Data in a,b,c,e,f are shown as the means +s.d. from at least 3 independent experiments.

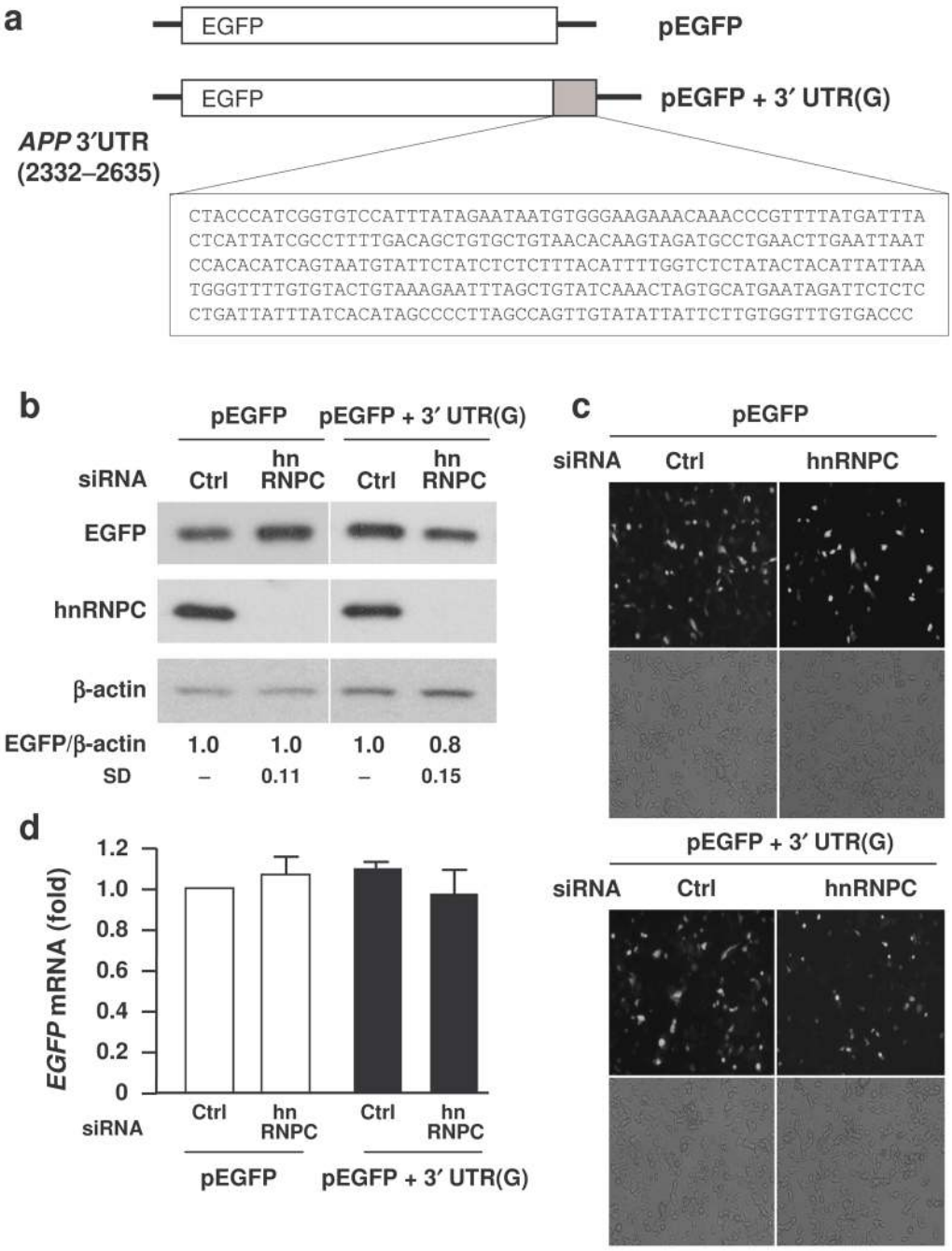

Figure 3. hnRNP C modestly reduces APP expression levels through APP 3′UTR

(a) Schematic of reporter plasmids pEGFP (control) and pEGFP + 3′ UTR(G), bearing the APP 3′UTR segment G (Fig. 1b). **(b)** By 48 h after transfection of either Ctrl or hnRNP C-directed siRNAs, together with each reporter plasmid, the levels of EGFP, hnRNP C, and loading control β-actin were assessed by Western blot analysis and quantified by densitometry. **(c)** EGFP signals in the transfection groups described in (b) were visualized by fluorescence microscopy. **(d)** In cells that were processed as described in (b), the levels of *EGFP* and *EGFP + 3′ UTR(G)* mRNAs in the transfection groups were measured by RT-qPCR and plotted relative to *EGFP* mRNA levels in Ctrl siRNA cells. The data in (b) and (c) represent the means +s.d. from 3 independent experiments.

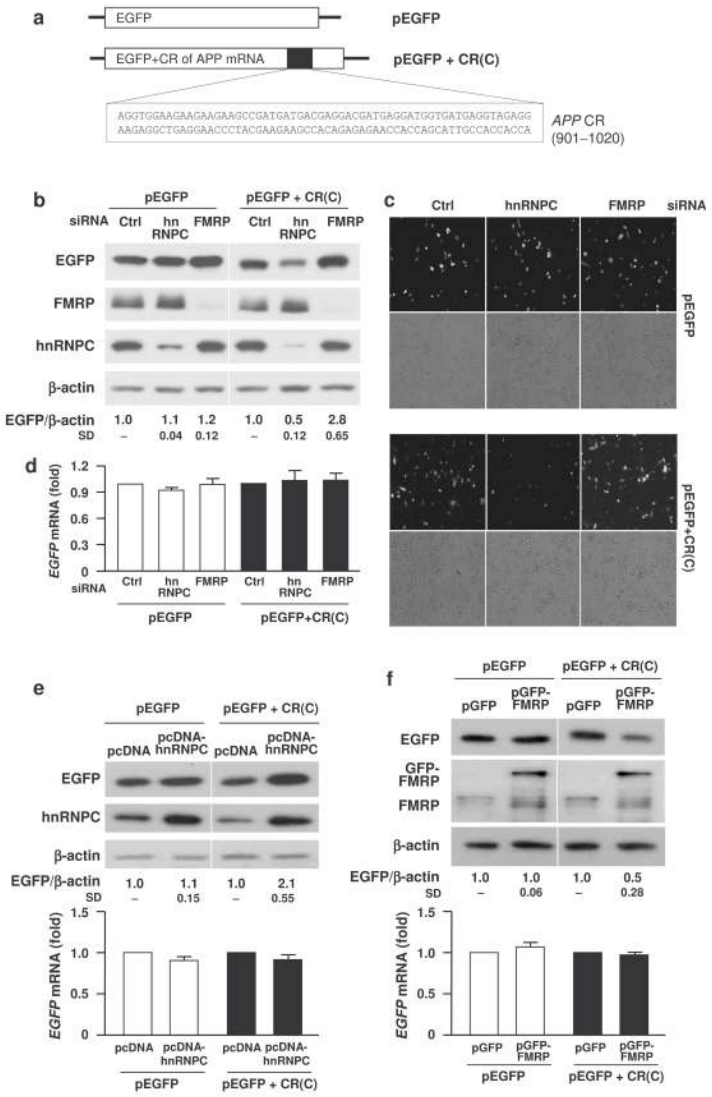

Figure 4. hnRNP C and FMRP control APP levels through the *APP* CR(C)

(a) Schematic of reporter plasmids pEGFP (control) and pEGFP + CR(C), bearing the *APP* CR segment C (Fig. 1b). **(b)** By 48 h after transfection of either Ctrl, hnRNP C-directed, or FMRP-directed siRNAs, together with each reporter plasmid, the levels of EGFP, hnRNP C, FMRP and loading control β-actin were assessed by Western blot analysis and quantified by densitometry. **(c)** EGFP signals in the transfection groups described in (b) were visualized by fluorescence microscopy. **(d)** In cells that were processed as described in (b), the levels of *EGFP* and *EGFP + CR(C)* mRNAs in the transfection groups were measured by RT-qPCR. **(e)** Cells were co-transfected with control or hnRNP C overexpression vectors and with pEGFP or pEGFP + CR(C); 24 h later, the levels of EGFP, hnRNP C, and loading control β-actin were studied by Western blot analysis and quantified by densitometry (*top*) and the levels of *EGFP* and *EGFP + CR(C)* mRNAs by RT-qPCR (*bottom*). **(f)** Cells were co-transfected with control or FMRP overexpression plasmids and with pEGFP or pEGFP + CR(C); 24 h later the levels of EGFP, FMRP, and loading control β-actin were studied by Western blot analysis and quantified by densitometry (*top*) and the levels of *EGFP* and *EGFP + CR(C)* mRNAs by RT-qPCR (*bottom*). The data in (b,d,e,f) represent the means +s.d. from 3 independent experiments.

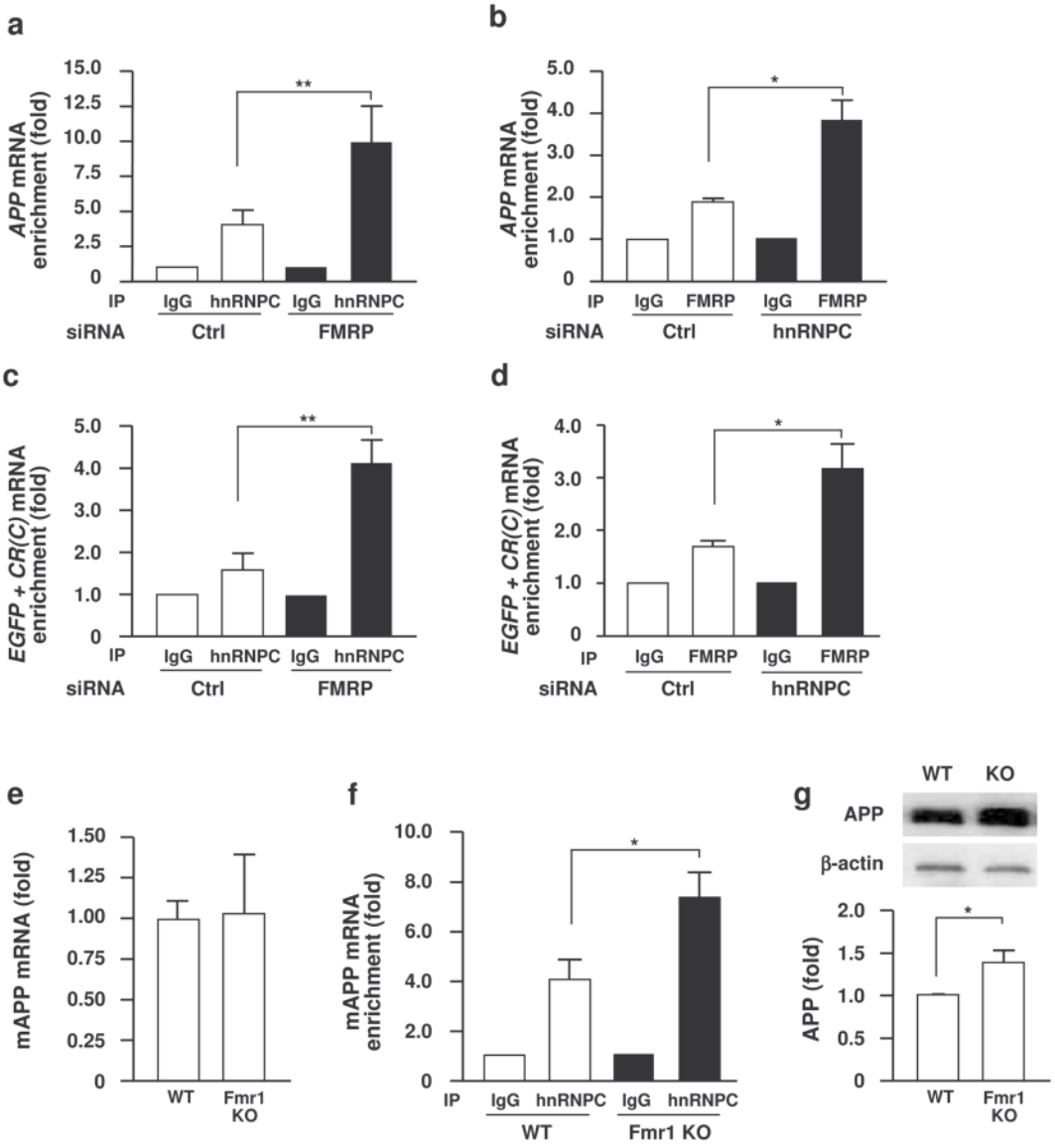

Figure 5. hnRNP C and FMRP bind the *APP* CR(C) competitively

(a) By 48 h after transfection of Ctrl or FMRP siRNAs, the association of *APP* mRNA with hnRNP C in each transfection group was measured by RNP IP followed by RT-qPCR analysis. **(b)** 48 h after transfection of Ctrl or hnRNP C siRNAs, the association of *APP* mRNA with FMRP in each transfection group was measured by RNP IP followed by RT-qPCR analysis. **(c)** By 48 h after transfection of pEGFP + CR(C) along with Ctrl or FMRP siRNAs, the levels of reporter *EGFP + CR(C)* chimeric mRNA associated with hnRNP C were measured by RNP IP followed by RT-qPCR analysis. **(d)** By 48 h after transfection of pEGFP + CR(C) together with Ctrl or hnRNP C siRNAs, the levels of *EGFP + CR(C)* chimeric mRNA associated with FMRP were measured by RNP IP followed by RT-qPCR analysis. Data are the means and +s.d. from 3 independent experiments. *, $p<0.05$; **, $p<0.01$. **(e)** RT-qPCR analysis of mAPP mRNA levels in whole-brain RNA preparations from WT and Fmr1 KO mice. **(f)** RNP IP analysis of mAPP mRNA enrichment in hnRNP C IP compared with IgG IP in WT and Fmr1 KO brain lysates. **(g)** *Top*, Western blot analysis of mAPP abundance in WT and Fmr1 KO

brain lysates; *bottom*, densitometric quantification of mAPP signals. Data in (e–g) represent the means +s.d. from 5 mice per group; *, $p<0.05$.

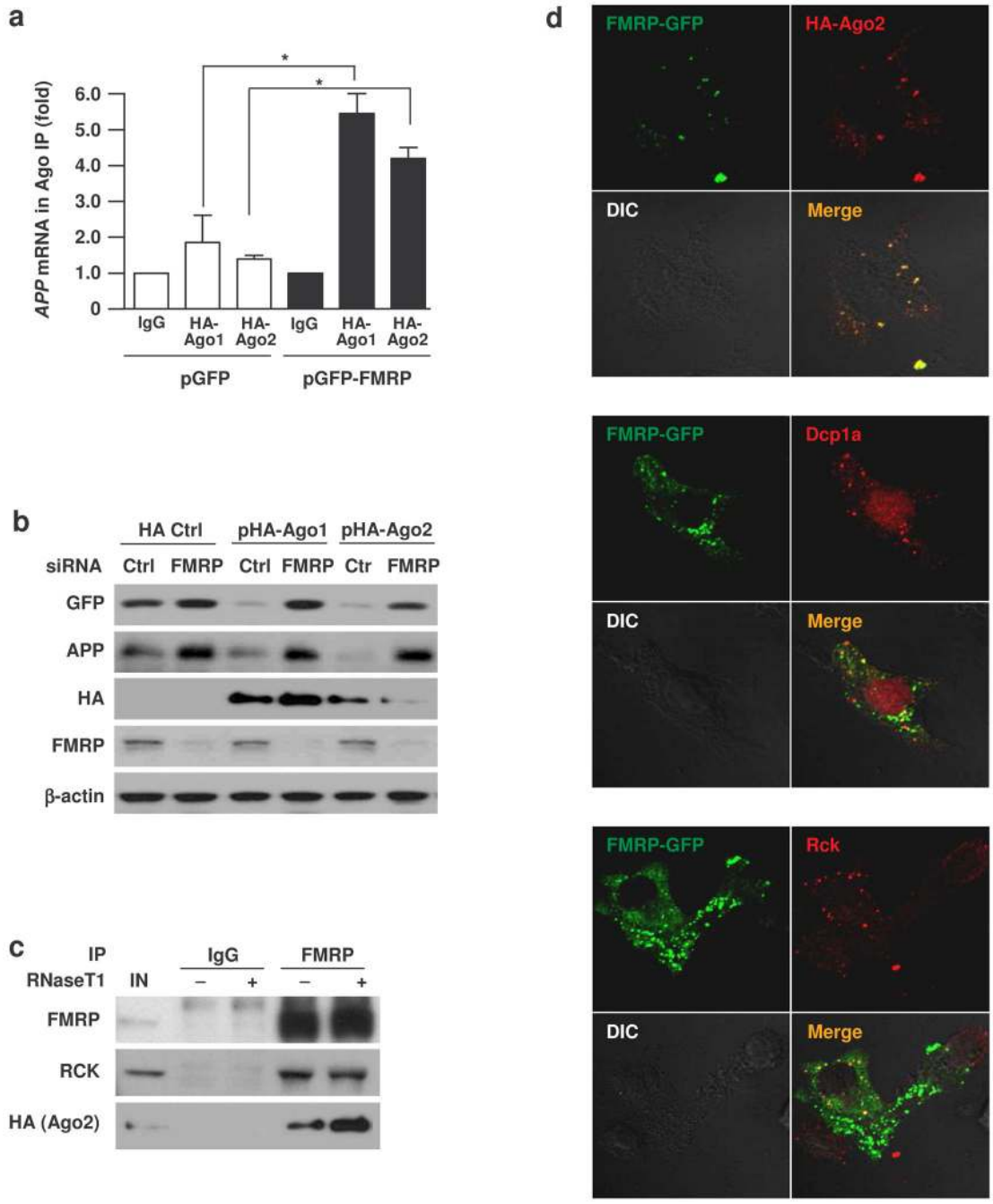

Figure 6. APP mRNA interacts with components of processing bodies

(a) By 24 h after transfection of pEGFP or pGFP-FMRP, the association of *APP* mRNA with HA-Ago1 or HA-Ago2 was measured by RNP IP using anti-HA or control IgG antibodies, followed byRT-qPCR analysis. Data represent the means +s.d. from three independent experiments. *, $p<0.05$. **(b)** By 24 h after silencing of FMRP (or leaving FMRP levels unchanged), plasmids pHA-Ago1 and pHA-Ago2 were co-transfected individually in order to overexpress Ago1 or Ago2. 24 h later, the levels of GFP, APP, HA-tagged proteins, FMRP and loading control β-actin were studied by Western blot analysis. **(c)** 24 h after transfection of pHA-Ago2, immunoprecipitation of protein complexes were performed on intact lysates (−) or lysates that had been incubated with RNaseT (+), using IgG or anti-FMRP antibodies.

The levels of FMRP, RCK, and HA-tagged proteins were studied by Western blot analysis. **(d)** Fluorescence analysis of FMRP colocalization with HA-Ago2 (*top*), Dcp1a (*middle*), and Rck (*bottom*). Red, antibodies detecting HA, Dcp1a, Rck; green, GFP; yellow, merging of the two signals. *DIC*, differential interference contrast.

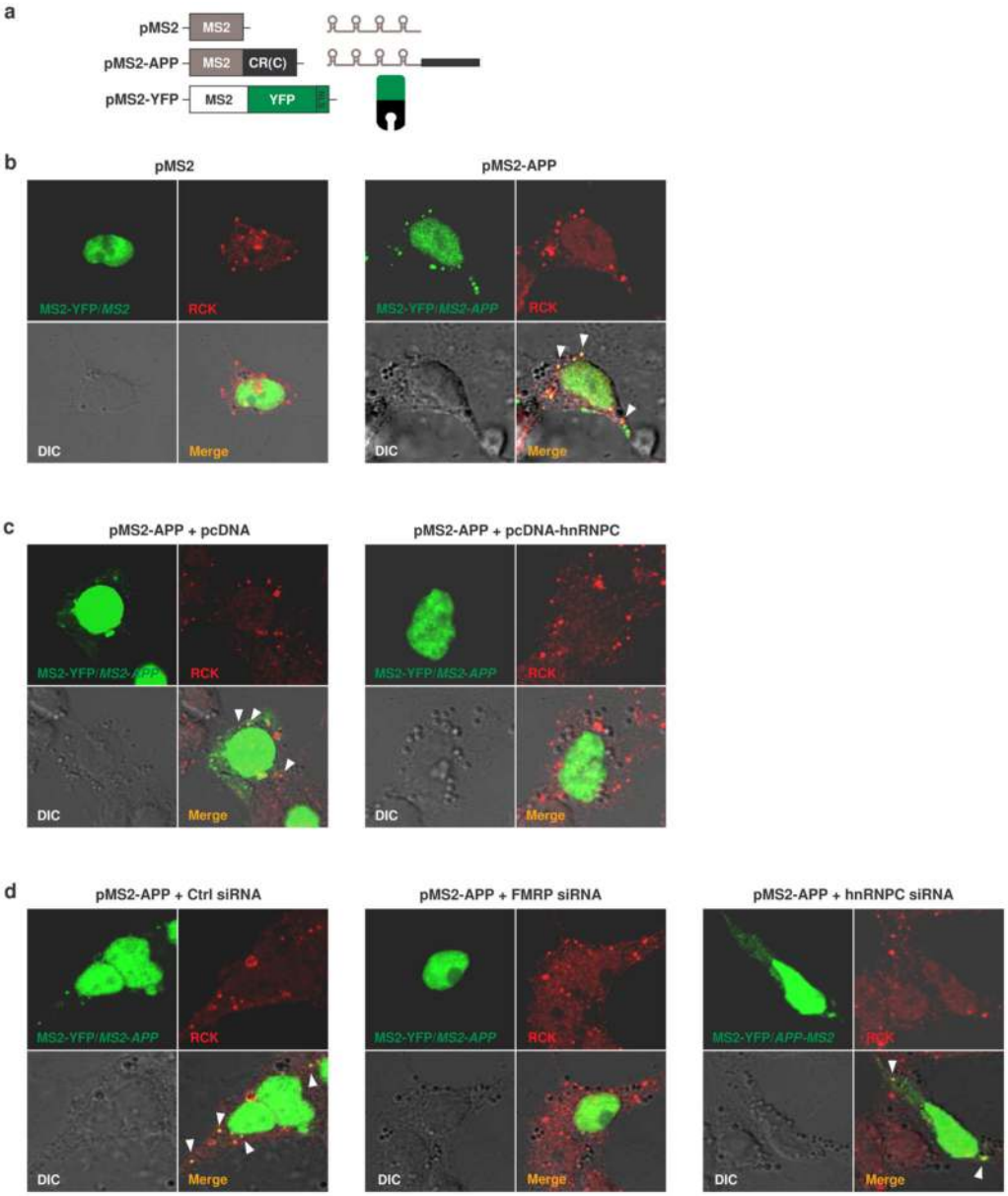

Figure 7. APP RNA colocalizes with PBs in an FMRP- and hnRNP C-dependent manner

(a) Schematic of the plasmids used for the visualization of APP RNA (see Methods). pMS2 and pMS2-APP (derived from pSL-MS2(24X)), expressed *MS2* and *MS2-APP* RNAs, each containing 24 tandem MS2 hairpins; pMS2-YFP expressed a fusion fluorescent protein (MS2-YFP) capable of detecting MS2-containing RNA. NLS, nuclear localization signal. **(b)** Using confocal microscopy, *MS2* (*left*) and *MS2-APP* (*right*) RNAs, visualized using MS2-YFP (*green* fluorescence), and RCK signals (*red* immunofluorescence) were detected and colocalized (*yellow*). **(c)** *MS2-APP* RNA was detected as explained in (b), in cells overexpressing hnRNP C (*right*) or transfected with the corresponding control vector (*left*). **(d)** *MS2-APP* RNA was detected as explained in (b) in cells transfected with siRNAs to lower hnRNP C (*right*), FMRP (*center*), or with control siRNA (*left,* shown also in Supplementary Fig. 7). siRNA and plasmid transfections were carried out as explained in the legend of Fig. 2. Blind scoring of cells in (b–d) revealed 100% of cells without cytoplasmic green/yellow signals in the pMS2, pMS2-APP + pcDNA-hnRNPC, or pMS2-APP + FMRP siRNA

transfection groups. In pMS2-APP, pMS2-APP + pcDNA, pMS2-APP + Ctrl siRNA, and pMS2-APP + hnRNPC siRNA populations, 60% of cells had yellow signals, indicating colocalization of tagged *APP* RNA and PBs (arrowheads).

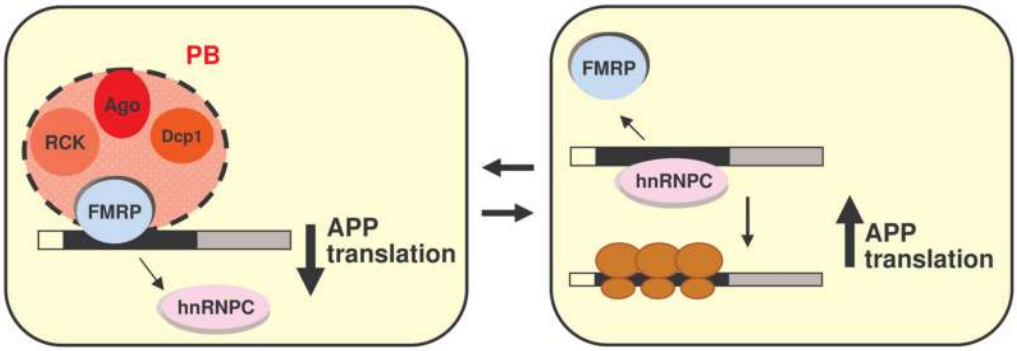

Figure 8. Model of competition between FMRP and hnRNP C to modulate APP translation

[AU: please insert title]Schematic representation of the proposed competition by FMRP and hnRNP C on the *APP* CR. As shown, the enhanced interaction of FMRP with *APP* CR reduces APP translation by recruiting the APP mRNA to PBs, while the increased association of hnRNP C increases APP translation. We hypothesize that the rate of APP biosynthesis is directly influenced by the relative association of each RBP.